Table 1. Characteristics of the computed cases.

Case	γ	Flux*	Grid†
a	20/17	0.125	20 × 20 × 37
b	20/17	0.125	20 × 20 × 46
c	20/17	0.333	20 × 20 × 46
d	5/3	0.125	20 × 20 × 37

*Dimensionless in the numerical simulation. †Number of mesh points: horizontal × horizontal × vertical.

($>H$) away from the top or bottom boundaries are plotted here to avoid contamination by boundary effects (at both ends, the vertical velocities are forced to vanish by the boundary conditions). All the points lie close to a straight line. However, the intercept of this line with the vertical axis is not zero; there is some residual velocity even when $\Delta\nabla$ approaches zero. The slope of the straight line is close to 1. Similarly, one would expect from Eq. 3 that T'/T varies linearly with $\Delta\nabla$ if α is constant. The temperature ratio is plotted versus the superadiabatic gradient in Fig. 4, which looks very similar to Fig. 3. The slope for these relations would also be close to 1. These results reinforce the validity of assuming that the mixing-length is proportional to the pressure scale height; they also demonstrate the feasibility of directly relating the mean dynamics to the mean atmospheric structure by simple relations similar to those given by the local MLT, in the limit that the convection is deep and efficient. Finally, the correlation, $C(V_z,\Delta T)$ is constant and has a value of about 0.8. Therefore, with Eq. 1, one can calculate the flux from a knowledge of $\Delta\nabla$, or vice versa.

The above results indicate that some basic assumptions made in computing coarse features of convection by means of MLT are valid, at least in the limited parameter range in which our numerical simulations were performed. However, one should not consider our results as a blanket confirmation of MLT. First, the parameter range of our computation does not cover all possible situations; for example, the values of the superadiabatic gradient are much smaller than those expected in the convective-radiative transition-layers where convection becomes less efficient but MLT is needed most. Second, much detailed dynamical information obtained by our simulation cannot be predicted by MLT. Consequently, problems that are sensitive to these details are not properly addressed by the MLT approach.

REFERENCES AND NOTES

1. L. Biermann, *Z. Astrophys.* **5**, 117 (1932).
2. E. Vitense, *ibid.* **32**, 135 (1953).
3. I. Iben, in *Stellar Evolution*, H. Y. Chiu and A. Muriel, Eds. (MIT Press, Cambridge, 1972), pp. 1–106.
4. F. Meyer and E. Meyer-Hofmeister, *Astron. Astrophys.* **106**, 34 (1982).
5. P. H. Stone, in *Jupiter*, T. Gehrels, Ed. (Univ. of Arizona Press, Tucson, 1976), pp. 587–618.
6. D. Gough and E. A. Spiegel, in *Problems of Stellar Convection*, E. A. Spiegel and J. P. Zahn, Eds. (Springer-Verlag, New York, 1977), pp. 57–62.
7. J. P. Cox and R. T. Giuli, *Principles of Stellar Structure* (Gordon and Breach, New York, 1968), pp. 281–325.
8. E. J. Opik, *Publ. Astron. Obs. Univ. Tartu* **301**, No. 3, (1938).
9. M. Schwarzschild, *Astrophys. J.* **134**, 1 (1961).
10. K. L. Chan and C. L. Wolff, *J. Comput. Phys.* **47**, 109 (1982).
11. K. L. Chan and S. Sofia, *Astrophys. J.* **307**, 222 (1986).

12. This research was partially supported by the National Science Foundation (grant AST-8504399). K.L.C. expresses his gratitude to P. Pesch for his encouragement.

28 August 1986; accepted 8 December 1986

The Glucocorticoid Receptor Protein Binds to Transfer RNA

MASARRAT ALI AND WAYNE V. VEDECKIS

The glucocorticoid receptor from mouse AtT-20 cells exists in three forms: (i) the untransformed receptor (9.1*S*; M_r of 319,000), a large oligomeric molecule that does not bind to DNA; (ii) the transformed receptor (4*S*; M_r of 96,000), which is formed by dissociation of untransformed receptor after steroid binding and which binds to DNA to modulate gene expression; and (iii) an intermediate size receptor (6*S*; M_r of 132,000), which also binds to DNA and contains a bound small RNA molecule. This RNA species has now been purified and identified as transfer RNA (tRNA). The three tRNA's for the basic amino acids accounted for about 78% of the total amino acid–accepting activity [arginine (52%), lysine (17%), and histidine (9%)], while the remaining 22% was represented by six other tRNA species. This tRNA-binding activity of the glucocorticoid receptor may reflect post-transcriptional mechanisms of regulating gene expression, such as alterations in the translational efficiency of or the modulation of the stability of hormone-induced proteins.

ALTHOUGH THE UNTRANSFORMED glucocorticoid receptor (GR) from mouse AtT-20 cells (*1–5*) contains no detectable bound RNA (*6*), RNA-binding activity has been demonstrated for the transformed estrogen (*7–9*), progesterone (*7*), androgen (*7, 10*), vitamin D (*10, 11*), and glucocorticoid (*4–7, 12–14*) receptor proteins [reviewed in (*3*)]. Thus, it appears that dissociation of subunits from the untransformed complex leads to the formation of the monomeric 4*S* GR (*2*) and the monomeric GR subsequently binds to small RNA molecules in the cytosolic extract, leading to formation of the 6*S* RNA–containing GR form. We have previously been able to reconstitute the 6*S* GR from partially purified 4*S* GR monomer and RNA (*4*). We therefore used the conversion of the 4*S* GR monomer to the 6*S* form by the addition of exogenous RNA as an assay for purification of this RNA.

RNA capable of shifting the 4*S* monomeric GR to 6*S* on sucrose gradients was purified by DEAE-cellulose chromatography, hydroxylapatite chromatography, sucrose gradient ultracentrifugation, and selection for RNA that was not polyadenylated on oligo dT–cellulose. The purified RNA [PIVB RNA: pool IV from DEAE-cellulose (eluted at 0.35*M* to 0.45*M* KCl), B (4*S*) pool from preparative sucrose gradients; see Fig. 1] was indistinguishable in size from yeast transfer RNA (tRNA) (mixture of several tRNA's) or purified *Escherichia coli* tRNA specific for valine or glutamic acid when analyzed on ethidium bromide–stained agarose gels. PIVB RNA was also indistinguishable from tRNA in its sedimentation coefficient (4*S*) on sucrose gradients. We treated the purified PIVB RNA preparation with calf intestinal alkaline phosphatase and then labeled it at the 5′ end with ^{32}P using polynucleotide kinase. We obtained three predominant ^{32}P-labeled bands—74 (minor), 76 (major), and 78 (minor) nucleotides (Fig. 1). Detectable amounts of ^{32}P-labeled RNA that were both larger and smaller than these species were also present. The fact that we could label the PIVB RNA demonstrated that it was not capped and, therefore, was not an RNA polymerase II transcript.

Several characteristics of PIVB RNA suggested that it contained tRNA: its size (76 nucleotides), the 4*S* sedimentation coefficient, the large amount obtained from the

Department of Biochemistry and Molecular Biology, Louisiana State University Medical Center, New Orleans, LA 70112.

cells (about 2 mg of RNA per 8 ml of packed cell volume), its cytoplasmic origin, and the fact that it could be 5′-end labeled after phosphatase treatment. Therefore, we incubated PIVB RNA with a mixture of [^{3}H]amino acids in the presence of rabbit liver tRNA synthetase to determine if the RNA could be aminoacylated. We also carried out this charging reaction with [^{35}S]methionine. These experiments clearly showed that PIVB RNA could be aminoacylated and, therefore, contained tRNA. Indeed, the amino acid–accepting activity of PIVB RNA was two to three times higher than that for cognate tRNA from rabbit liver.

After removal of the free amino acids and proteins by phenol-chloroform extraction and ethanol precipitation, the RNA was treated with alkali to liberate covalently attached [^{3}H]amino acids. After removal of the intact RNA by Sephadex G-25 chromatography, the nature of the amino acids present was determined with an amino acid analyzer (Fig. 2). We could identify nine amino acids that were released after hydrolysis of the aminoacylated PIVB RNA. On the basis of the recoveries of the individual [^{3}H]amino acids, we concluded that the relative composition of the aminoacylated PIVB RNA was: arginine (52%), lysine (17%), histidine (9.2%), threonine (6.2%), valine (5.1%), aspartic acid (4.8%), alanine (3.1%), phenylalanine (2.5%), and methionine (<0.1%). We do not yet know whether these values reflect the relative concentrations for the cognate tRNA species, the efficiency of the charging reaction for these particular amino acids, or both.

These experiments showed that tRNA molecules are present in the PIVB RNA that binds to the mouse GR. However, we had not yet determined whether the GR binds equivalently to all tRNA species. Indeed, about 500 RNA molecules were required to completely shift one GR protein from 4*S* to 6*S*, that is, to obtain stable formation of a GR-RNA complex on sucrose gradients (Fig. 3). Two explanations could be made for these results. First, a large excess of RNA may be required to maintain the receptor in a stable 6*S* GR-RNA complex under the nonequilibrium conditions of sucrose gradients. Second, a minor RNA species could bind specifically to the GR while the majority of the PIVB RNA (that is, tRNA) did not interact with the receptor. We therefore titrated the GR with various concentrations of PIVB RNA, as well as with glutamic acid–specific tRNA from *E. coli*.

Both PIVB RNA (5.6 μg) and *E. coli* tRNA^{glu} (5.6 μg) could completely shift the GR from 4*S* to 6*S* (Fig. 3). Half this amount (2.8 μg) of both RNA preparations caused a shift of about one-half of the GR to 6*S*, while 1.4 μg of *E. coli* tRNA^{glu} was incapable of shifting any of the GR to 6*S*. Similar results were obtained with purified *E. coli* tRNA^{val} and tRNA^{met} samples. These results suggest that it is the tRNA itself in PIVB RNA that interacts with the GR. It is not likely that a purified preparation of *E. coli* glutamic acid–specific tRNA (the amino acid acceptor activity for glutamic acid was 800 pmol per A_{260} unit; 0.006% contamination of tRNA for glycine, isoleucine, and valine) would contain a minor RNA (not tRNA) component that could interact specifically with the GR and that was identical to one that might have been in the PIVB RNA preparation. Finally, the GR is also capable of interacting with aminoacylated tRNA. PIVB RNA was charged with [^{3}H]amino acids and then mixed with the GR monomer. The GR was capable of shifting the 4*S* [^{3}H]aminoacyl-tRNA complex to 6*S* on sucrose gradients. Thus, the mouse GR appears to interact directly with the tRNA (PIVB RNA) we have purified from the mouse AtT-20 cells.

Thus the GR from mouse AtT-20 cells can bind to tRNA. The specificity of the GR-tRNA interaction has not yet been unequivocally established. It may be argued that the GR, by virtue of its affinity for DNA, may interact nonspecifically with any double-stranded nucleic acid (DNA, tRNA, 5*S* RNA, ribosomal RNA, and so forth). However, our evidence suggests that the GR shows more specificity for tRNA. For instance, 90% of the total cellular RNA (incapable of binding to the 4*S* GR to generate the 6*S* form) has been eliminated during the purification of PIVB RNA. Ribosomal RNA (which possesses secondary structure comparable to tRNA) and messen-

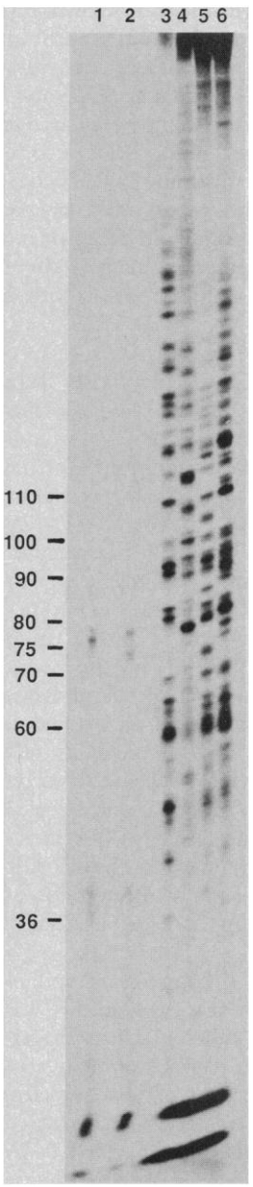

Fig. 1. Molecular size determination of PIVB RNA; 5′ end, ^{32}P-labeled PIVB RNA and yeast tRNA were analyzed on an acrylamide (6%) sequencing gel containing 8*M* urea. Lane 1, PIVB RNA; lane 2, yeast tRNA; lanes 3 to 6, four reactions performed for A, G, C, and T with the "dideoxy" sequencing method. The DNA sample was a Bam HI restriction fragment from the mouse c-*myb* gene. Lanes 3 to 6 were used to determine the size of the RNA samples. The RNA associated with the 6*S* GR was fractionated by DEAE-cellulose chromatography as described in Fig. 3. The bound RNA was eluted with a linear 0*M* to 1*M* KCl gradient and monitored by the absorbance at 260 nm. Fractions eluting after the GR were pooled into seven pools of five consecutive fractions. These pools were tested for their ability to shift the 4*S* monomeric GR to 6*S*. Only fractions eluting between 0.35*M* and 0.45*M* KCl (PIV and PV) were capable of reconstituting the 6*S* GR. These fractions were loaded onto a hydroxylapatite (HAP) column and eluted with a phosphate gradient. The RNA that bound to HAP was pooled, extracted with phenol-chloroform, and precipitated with ethanol. This sample was loaded onto a 5 to 20% sucrose gradient and centrifuged. A single, sharp 4*S* peak (pool B) that absorbed at 260 nm was obtained. The peak fractions were pooled and passed over an oligo dT–cellulose column. The majority of the RNA did not absorb. The polyadenylated material was 11% of the starting RNA and was designated PIVB RNA. PIVB and yeast tRNA (control) were dephosphorylated with calf intestinal alkaline phosphatase (Boehringer). A typical reaction contained 10 μl of RNA (2 to 10 μg), 8 μl of alkaline phosphatase (1 unit/μl), and 1.8 μl of 10× buffer (500 m*M* tris-HCl, *p*H 8.0, and 1 m*M* EDTA). This was incubated at 55°C for 1 hour, extracted once with phenol-chloroform, and the RNA precipitated overnight at −20°C with 2.5 volumes of 95% ethanol. RNA was dissolved in water at a concentration of about 0.5 μg/μl and labeled at the 5′ end with T4 polynucleotide kinase (P-L Biochemicals). The first reaction step involved incubating 25 μCi of [γ-^{32}P]ATP (3000 Ci/mmol; New England Nuclear), 6.25 μl of 2× kinase buffer A (10 m*M* glycine, *p*H 9.5, 1 m*M* spermidine, and 100 m*M* EDTA), 3 μl of dephosphorylated RNA, and 3.25 μl of H_2O for 10 minutes at 65°C. Following this, 1 μl of kinase buffer B (1*M* glycine, *p*H 9.5, and 200 m*M* $MgCl_2$), 1 μl of 10 m*M* dithiothreitol, and 1 μl of T4 polynucleotide kinase (10 unit/μl) were added and the mixture then incubated for 2 hours at 37°C. Unreacted [^{32}P]ATP was removed by Sephadex G-25 gel filtration. The ^{32}P incorporation into PIVB RNA and yeast tRNA was about 17 pmol and 40 pmol, respectively.

ger RNA do not bind to the 4*S* GR to yield 6*S* complexes (*5*). The GR-RNA complexes exist in the nucleus and in intact cells under in vivo conditions (*12, 15, 16*). In addition the GR possesses distinct binding sites for DNA and RNA (*17*). We also found that PIVB RNA or tRNA did not affect the sedimentation coefficients of bovine serum albumin (a protein with an *S* value similar to the 4*S* GR) and chymotrypsinogen (a basic protein). Thus, not all proteins can interact with tRNA. On the basis of this evidence, it may be concluded that there probably exists some specificity, both at the level of the protein (GR) and the RNA (tRNA). However, tRNA samples (in a mixture or purified form) from a variety of species such as cow, rabbit, yeast, and *E. coli* were equally effective in generating the 6*S* GR when added to the 4*S* form. The lack of any species specificity for the tRNA indicates that a large degree of secondary or stem loop structure, common to all tRNA's, may be important for the interaction with the GR.

What significance might the GR-tRNA binding have? Although poorly understood, there are numerous reports of nongenomic effects of glucocorticoids, as well as of other steroid hormones (*18*). For example, the GR binding to tRNA might alter the efficiency of translation and this could modulate protein synthesis. Recently, substantial progress has been made in elucidating the mechanism involved in nonlysosomal, adenosine triphosphate (ATP)–dependent, ubiquitin-mediated protein degradation (*19*). Specifically, an ATP-dependent system that requires tRNA for activity causes the covalent attachment of ubiquitin to proteins (*20*). In addition, the charging of a specific tRNA ($tRNA^{his}$) has been shown to be necessary for the selective degradation of albumin (but not ribonuclease and lysozyme) (*21*). The abundance of the three basic amino acid tRNA species in purified PIVB RNA (Fig. 2) suggests that the GR could potentially operate through one of these tRNA molecules. The ubiquitination of proteins serves as a tag, leading to degradation of the ubiquitinated proteins. Thus, the GR could affect the expression of hor-

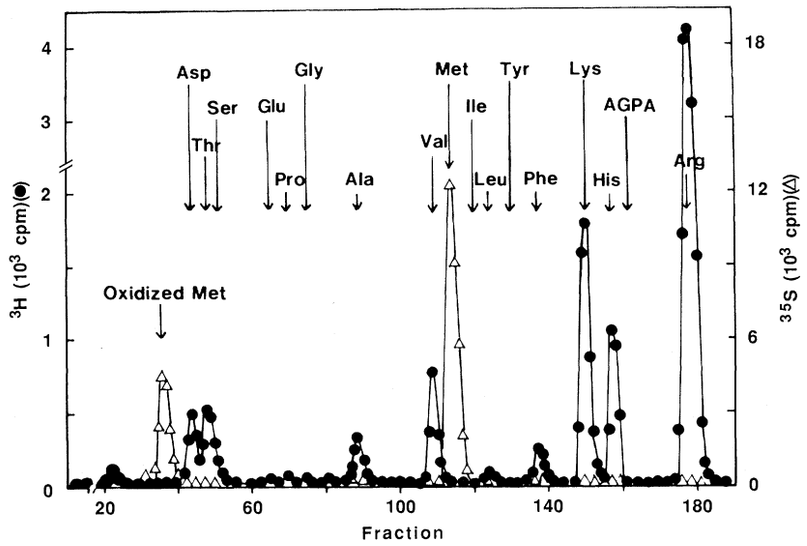

Fig. 2. Identification of tRNA species in PIVB RNA by aminoacylation. Tritiated amino acids were hydrolyzed from aminoacylated-tRNA after charging PIVB RNA with a mixture of tritiated amino acids and rabbit liver aminoacyl-tRNA synthetase. A separate reaction was performed with [^{35}S]methionine. The liberated amino acids were then detected with an amino acid analyzer and the appropriate standards. PIVB RNA (2.56 μg) was added to 5 μl of 10× charging reaction buffer (1*M* tris-HCl, 50 m*M* $MgCl_2$, 0.5*M* KCl, 5 m*M* EDTA, and 25 m*M* ATP, *p*H 7.6 at 37°C), 3 μl of [^{3}H]L-amino acid mixture (250 mCi/mg, ICN Radiochemicals), and H_2O to bring the final volume to 40 μl. This was incubated for 10 minutes at 37°C. Ten microliters of rabbit liver aminoacyl-tRNA synthetase (3 mg/ml, 7800 units per milligram of protein; Sigma) were added and the reaction allowed to proceed for 10 minutes at 37°C. Ten percent ice-cold trichloroacetic acid (TCA) was added and the precipitate collected under slight vacuum on filter paper disks. The filters were washed successively with 1 ml each of ice-cold 5% TCA, 5% TCA containing 0.1% of an unlabeled amino acid mixture, and finally a mixture of 5% TCA and 95% ethanol. The filters were then dried and the radioactivity measured by scintillation spectroscopy to determine amino acid incorporation into aminoacyl-tRNA. Replicate filters were trimmed and soaked in 300 μl of 0.01*N* NaOH with occasional shaking to liberate the hydrolyzed amino acids. The eluted material from several filters was pooled, freed of particulate matter by centrifugal filtration, and the filtrate neutralized with 0.1*N* HCl. Sephadex G-25 filtration of aliquots showed that hydrolysis was complete, as all of the radioactivity eluted in the included volume. The neutralized amino acid solution was dried and dissolved in 200 μl of 0.1*M* citrate buffer, *p*H 2.2. After the addition of a standard amino acid solution and α-aminoguanidinopropionic acid (AGPA) (to monitor the efficiency of the run), the sample was injected into an amino acid analyzer. Fractions (180 μl) were collected and the elution of the standards monitored as a function of retention time. The retention time (in minutes) for the standards were Asp/Asn (25.2), Thr (28.0), Ser (29.5), Glu/Gln (39.0), Pro (41.6), Gly (48.6), Ala (53.0), Val (65.9), Met (69.5), Ile (73.4), Leu (76.3), Tyr (80.6), Phe (83.2), Lys (90.8), His (96.2), AGPA (102.5), and Arg (109.3). Total run time was 120 minutes. The radioactivity in each fraction was measured to determine which aminoacylated-tRNAs were originally present in PIVB RNA.

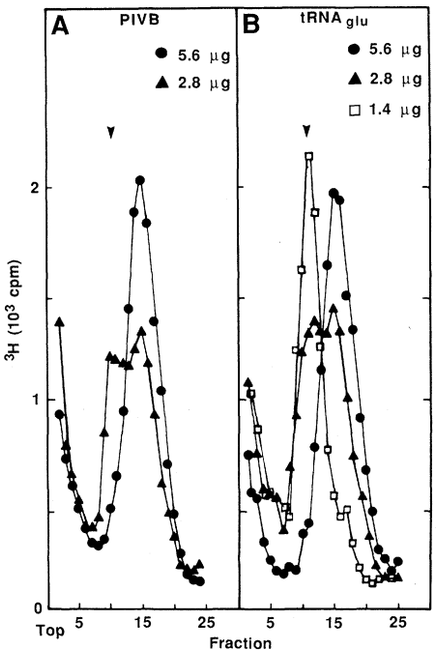

Fig. 3. PIVB RNA concentration dependent shift of the 4*S* GR to 6*S*. Monomeric, 4*S* transformed GR was mixed with (**A**) PIVB RNA or (**B**) *E. coli* glutamic acid–specific tRNA (Sigma) in a total volume of 90 μl for 5 minutes on ice. One hundred ten microliters of TETg (20 m*M* tris-HCl, 1 m*M* EDTA, and 12 m*M* 1-thioglycerol, *p*H 7.4, at 25°C) buffer was added and each sample run on a vertical tube rotor sucrose gradient (5 to 20%) at 2°C, 463,000g_{av}, to a preset cumulative centrifugal effect ($\omega^2 t$) of 3.04×10^{11} rad^2/sec. [^{14}C]Methylated chymotrypsinogen A (2.6*S*), ovalbumin (3.5*S*), aldolase (7.9*S*), and β-amylase (9.4*S*) were used as standards in a parallel tube to determine the sedimentation coefficient of the GR (*23*). Preparation of the monomeric, 4*S* transformed GR has been described (*2*). Briefly, AtT-20 cell cytosol (10 ml) was labeled overnight at 4°C with 2×10^{-8}*M* [1,2,4-^{3}H]triamcinolone acetonide (TA) (78 Ci/mmol; Amersham). The GR was transformed by filtration on a Sephadex G-25 column (*5, 6*) and incubation of the excluded volume fractions for 2 hours at 15°C and then 1 hour at 4°C. This preparation was applied to a DEAE-cellulose column and eluted with a 0*M* to 1*M* KCl gradient. The GR elutes at about 0.1*M* KCl. The peak fractions were pooled, desalted on a Sephadex G-25 column, and frozen in aliquots at −70°C. The GR in this preparation sediments at about 4*S* on low salt (TETg) 5 to 20% sucrose gradients. Addition of PIVB RNA or purified *E. coli* tRNA increases the sedimentation rate of the GR to about 6*S*. The gradients were fractionated and the radioactivity determined by scintillation spectroscopy to determine the position of the receptor-bound [^{3}H]TA. The arrowhead indicates the sedimentation position of 4*S* GR.

monally regulated proteins by modulating its own stability or modulating GR-mediated ubiquitination and subsequent degradation of other proteins. In fact, glucocorticoid hormone treatment has been shown to stimulate protein catabolism associated with muscle wasting (*22*). Because glucocorticoid hormone treatment results in a predominance of the transformed, monomeric GR capable of binding tRNA (as documented in our study), this GR may then participate in the ubiquitin pathway.

REFERENCES AND NOTES

1. W. V. Vedeckis, *Biochemistry* **22**, 1975 (1983).
2. ———, *ibid.*, p. 1983.
3. ———, in *Hormonally Responsive Tumors*, V. P. Hollander, Ed. (Academic Press, New York, 1985), pp. 3–61.
4. C. E. Reker, B. Kovačič-Milivojević, S. B. Eastman-Reks, W. V. Vedeckis, *Biochemistry* **24**, 196 (1985).
5. B. Kovačič-Milivojević *et al.*, *ibid.*, p. 7357.
6. B. Kovačič-Milivojević and W. V. Vedeckis, *ibid.*, in press.
7. S. Liao *et al.*, *J. Biol. Chem.* **255**, 5545 (1980).
8. M. T. Chong and M. E. Lippman, *ibid.* **257**, 2996 (1982).
9. T. Thomas and T. Kiang, *J. Steroid Biochem.* **23**, 19 (1985).
10. A. Haase, B. Ofenloch, K. Eisele, *Biochem. Int.* **7**, 541 (1983).
11. R. T. Franceschi, *Proc. Natl. Acad. Sci. U.S.A.* **81**, 2337 (1984).
12. I. V. Economidis and G. G. Rousseau, *FEBS Lett.* **181**, 47 (1985).
13. J. L. Tymoczko, M. M. Phillips, S. M. Vernon, *Arch. Biochem. Biophys.* **230**, 345 (1984).
14. E. E. Anderson and J. L. Tymoczko, *J. Steroid Biochem.* **23**, 299 (1985).
15. G. P. Rossini, *Biochem. Biophys. Res. Commun.* **123**, 78 (1984).
16. S. Liao, T. Liang, J. L. Tymoczko, *Nature (London) New Biol.* **241**, 211 (1973).
17. J. L. Tymoczko and J. H. Lee, *Biochim. Biophys. Acta* **846**, 193 (1985).
18. G. S. McKnight and R. Palmiter, *J. Biol. Chem.* **254**, 9050 (1979); D. M. Robins and R. T. Schimke, *ibid.* **253**, 8925 (1978).
19. A. Bachmair, D. Finley, A. Varshavsky, *Science* **234**, 179 (1986); D. Finley and A. Varshavsky, *Trends Biochem. Sci.* **10**, 343 (1985).
20. A. Ciechanover, S. L. Wolin, J. A. Steitz, H. F. Lodish, *Proc. Natl. Acad. Sci. U.S.A.* **82**, 1341 (1985); S. Ferber and A. Ciechanover, *J. Biol. Chem.* **26**, 3128 (1986).
21. O. A. Scornik, *J. Biol. Chem.* **258**, 882 (1983).
22. M. Mayer, in *Intracellular Protein Catabolism*, E. A. Khairallah, J. S. Bond, J. W. C. Bird, Eds. (Liss, New York, 1985), pp. 543–554.
23. S. B. Eastman-Reks, C. E. Reker, W. V. Vedeckis, *Arch. Biochem. Biophys.* **230**, 274 (1984).

24. Supported by NIH grant AM-36086 (to W.V.V.), Cancer Crusaders, and Tri Golf Parish, LA (to M.A.). W.V.V. is the recipient of an NIH Research Career Development Award. We thank W. T. Morgan for assistance with the amino acid analysis, D. K. Sheiness for assistance with the DNA sequencing gel, and P. L. Deininger for many helpful suggestions and discussions.

28 July 1986; accepted 24 November 1986

Brain Barrier Tissues: End Organs for Atriopeptins

LUCA STEARDO* AND JAMES A. NATHANSON†

Little is known about the pathophysiology of cerebral edema and other disturbances of water balance that involve the barrier tissues at the interface of blood and brain. The present experiments show that these barrier tissues contain receptors and second messenger systems for atriopeptins, recently identified cardiac peptides involved in peripheral water regulation. They also show that atriopeptins can alter the rate of cerebrospinal fluid production. Because the blood-brain and blood–cerebrospinal fluid barriers are involved in normal water movements in the central nervous system, these studies suggest that brain barrier tissues may be important end organs for the atriopeptins and that atriopeptins could have therapeutic application to disorders of water balance in the central nervous system. An isolated, purified population of atriopeptin receptor cells, obtained from choroid epithelium, was used in these experiments. This cell population may provide a valuable model system for investigating the intracellular biochemical mechanisms through which atriopeptins exert their actions.

BECAUSE THE BRAIN IS ENCASED within a rigid skull and lacks a true lymphatic drainage system, it is critically vulnerable to damage from edema. However, when compared with peripheral tissues, relatively little is known about intracranial regulation of water and electrolytes. Extracellular fluid movement into and out of the brain occurs primarily at the blood-brain barrier (capillary endothelium), blood–cerebrospinal fluid (CSF) barrier (choroid plexus epithelium), and CSF outflow system (dural sinus–arachnoid villi) (*1*). Recently, it became apparent that atriopeptins, released from atrial cardiocytes, may be key hormones for regulating fluid volume in the periphery (*2*). Because the endothelial cells of the blood-brain barrier and the epithelial cells of the blood-CSF barrier potentially have access to circulating atriopeptins, we investigated the possibility that brain barrier tissues might be end organs for atriopeptins. Our biochemical and physiological studies, detailed below, support this possibility (*3*). We also describe a cell population that may be useful for studying the mechanisms of action of atriopeptin receptors both in the brain and periphery.

Evidence from peripheral tissues suggests that atriopeptin receptor occupancy is associated with the intracellular production of guanosine 3′,5′-monophosphate (cyclic GMP) (*4*). Therefore, to determine whether atriopeptin receptors might be present in brain barrier tissues, we first attempted to establish whether atriopeptin-activated guanylate cyclase activity could be demonstrated in washed membrane fractions prepared from these tissues. The presence of such activity would indicate that these peptides not only bind to the membrane but that they are capable of exerting a biochemical alteration of membrane activity.

Figure 1A shows that rat atrial natriuretic peptide (rANP) 1–28 (Ser-Leu-Arg-Arg-atriopeptin III) was a potent activator of guanylate cyclase activity in purified rabbit cerebral microvessels [maximum velocity of enzyme activity (V_{max}), 215% of control; activation constant (K_a), 0.5 n*M*]. From other studies, it is known that such microvessels consist of a high percentage of endothelial cell–containing cerebral capillaries (*5*). A similar degree of activation of guanylate cyclase by rANP was observed in microvessels prepared from pig brain.

Figure 1B (middle curve) shows that rANP also stimulated enzyme activity in membrane fractions prepared from whole rabbit choroid plexus obtained from lateral, third, and fourth ventricles. In five separate experiments, the K_a for activation of the enzyme in the choroid (9.8 ± 5.1 n*M*; SEM) was similar to that (K_a = 5 ± 2 n*M*; SEM, n = 4) which we observed in rabbit kidney, a tissue known to be rich in atriopeptin receptors (*4, 6*), and somewhat greater than that which we observed for atriopeptin stimulation in the rabbit cerebellum (Fig 1A), a tissue known to be enriched (relative to other brain areas) in cyclic GMP (*7*). The V_{max} for stimulation of basal activity in the choroid plexus averaged 58% ± 16% (SEM, n = 5).

However, we found no stimulation of guanylate cyclase activity in membrane fractions prepared from rabbit or pig cerebral cortex (Fig. 1A). In membranes prepared from the ventral portion of pig or rabbit superior sagittal dural sinus, which contains

Department of Neurology, Harvard Medical School, and Neuropharmacology Research Laboratory, Massachusetts General Hospital, Boston, MA 02114.

*Present address, Department of Neurology, University of Naples, Naples, Italy.
†To whom correspondence should be addressed.